

Fig. 3 Closed-loop responses for two "distinctly different" optimal solutions for case 2.

0.33L, 0.33L and 0.66L, and 0.66L and 1.0L, respectively. The coding used for this study is shown below:

10 bits each	10 bits each
1011100010...	1000010111...
Position gains	Velocity gains
10 bits each	10 bits each
0001111011...	1101111011...
Actuator locations	Sensor locations

## Results

The technique outlined above was used to solve the two optimization cases presented earlier. Reference 9 includes detailed presentation of the numerical results obtained for the two cases. Figure 2 presents plots of the final population solution for cases 1 and 2. In Fig. 2, the  $x$  axis represents an actuator location norm defined as  $x/L = x/L$  for case 1 and  $x/L = (1/L)(x_{A1}/0.33 + x_{A2}/0.66 + x_{A3}/0.99)$  for case 2. The  $y$  axis represents a normalized performance measure, with zero indicating the best solution found by the GA. It is evident from these figures that for the one-actuator, one-sensor case the local optimum is the global optimum. However, for the three-actuator, three-sensor case, three distinct optimal points were found. These optimal points are marked in Fig. 2b. Figure 3 presents closed-loop responses for optimal solutions 1 and 3, as noted in Fig. 2b. Although the actuator locations differ significantly, the closed-loop responses are similar.

## Conclusions

This Note has proposed two unique ideas in the realm of optimization for structural control: 1) simultaneous actuator/sensor placement and feedback controller gain optimization and 2) finding more than one "distinctly different" near-optimal solution. To implement these ideas, a genetic algorithm optimization technique was used. For the multiple optimal solutions, we induced niche formation in a genetic algorithm using a sharing mechanism. The end result is the convergence of the genetic algorithm population to multiple locally near-optimal solutions. The concepts were demonstrated using a simple clamped-free beam.

## References

- <sup>1</sup>Lindberg, R. E., and Longman, R. W., "On the Number and Placement of Actuators for Independent Modal Space Control," *Journal of Guidance and Control*, Vol. 7, No. 2, 1984, pp. 215–221.
- <sup>2</sup>Rao, S. S., Pan, T., and Venkayya, V. B., "Optimal Placement of Actuators in Actively Controlled Structures Using Genetic Algorithm," *AIAA Journal*, Vol. 29, No. 6, 1991, pp. 942, 943.
- <sup>3</sup>Montgomery, L., KrishnaKumar, K., and Weeks, G., "Structural Control Using Connectionist Learning Principles," AIAA Paper 92-4467.
- <sup>4</sup>Chang, I. J., and Soong, T. T., "Optimal Controller Placement in Modal Control of Complex Systems," *Journal of Mathematical Analysis and Applications*, Vol. 75, 1980, pp. 340–358.
- <sup>5</sup>Choe, K., and Baruah, A., "Actuator Placement in Structural Control," *Journal of Guidance, Control, and Dynamics*, Vol. 15, No. 1, 1992, pp. 40–48.

<sup>6</sup>KrishnaKumar, K., and Goldberg, D. E., "Genetic Algorithms in Control System Optimization," *Journal of Guidance, Control, and Dynamics*, Vol. 15, No. 3, 1992, pp. 735–740.

<sup>7</sup>Goldberg, D. E., *Genetic Algorithms in Search Optimization and Machine Learning*, Addison-Wesley, Reading, MA, 1989.

<sup>8</sup>Deb, K., "Genetic Algorithms in Multimodal Function Optimization," M.S. Thesis, College of Engineering, Univ. of Alabama, Tuscaloosa, AL, 1989.

<sup>9</sup>KrishnaKumar, K., Swaminathan, R., and Montgomery, L., "Multiple Optimal Solutions for a Structural Control Problem Using a Genetic Algorithm with Niching," AIAA Paper 93-3873.

## Measures of Modal Controllability and Observability in Vibration Control of Flexible Structures

Zhong-sheng Liu,\* Da-jun Wang,\* Hai-chang Hu,\* and Min Yu\*

Peking University, Beijing 100871,  
People's Republic of China

## Introduction

A COMPLEX issue in the control of large flexible space structures is that there may exist repeated or closely spaced modes clumping together in the lower range of the natural frequency spectrum. In practice, only a few modes can be selected for control because of the limited capacity of the hardware. One of the criteria for mode selection is modal controllability and observability. Thus it is desirable to have a method to evaluate the modal controllability and observability quantitatively. Reference 1 investigated the modal controllability and observability for distinct modes. References 2–4 proposed criteria for the controllability and observability of repeated modes, which are, however, not quantitative. References 5 and 6 addressed the model reduction problem based on the singular values of the controllability and observability grammians. The new idea of the present paper is the use of the singular-value decomposition of the input matrix  $B_0$  in defining controllability. This approach is also presented for observability on the basis of duality. It is suitable for both distinct and repeated modes. Using this technique, modal controllability and observability can be quantitatively measured by the associated singular values. In the case of repeated frequency modes, the present method can generate two new groups of orthogonal principal vectors that span the eigensubspace associated with the repeated modes. These principal vectors are ordered in the sequence of their controllability and observability measures.

## Background

Consider a linear, time-invariant, second-order control system

$$M\ddot{x} + Kx = Bu(t) \quad (1a)$$

$$y = Cx(t) \quad (1b)$$

where  $M = M^T \in R^{n \times n}$ ,  $K = K^T \in R^{n \times n}$ ,  $B \in R^{n \times p}$ ,  $C \in R^{l \times n}$ ,  $x(t) \in R^n$ ,  $u(t) \in R^p$ , and  $y \in R^l$ . Matrices  $B$  and  $C$  are called the actuator distribution matrix and sensor distribution matrix, respectively, indicating the locations of control forces and sensors, respectively. Mass matrix  $M$  and stiffness matrix  $K$  are assumed to be positive definite.

Transforming Eq. (1) to the modal coordinates through the coordinate transformation

$$x(t) = \Phi\eta(t) \quad (2)$$

Received May 19, 1993; revision received Jan. 14, 1994; accepted for publication Jan. 20, 1994. Copyright © 1994 by the American Institute of Aeronautics and Astronautics, Inc. All rights reserved.

\*Department of Mechanics.

yields

$$\ddot{\eta}(t) + \Lambda \eta(t) = \Phi^T B u(t) \quad (3a)$$

$$y = (C \Phi) \eta(t) \quad (3b)$$

where  $\Phi \equiv [\varphi_1, \varphi_2, \dots, \varphi_n]$ ,  $\Lambda \equiv \text{diag}[\omega_1^2, \omega_2^2, \dots, \omega_n^2]$  are the eigensolutions of the eigenproblem

$$K \varphi_i = \omega_i^2 M \varphi_i \quad (4a)$$

$$\varphi_i^T M \varphi_i = 1, \quad i = 1, 2, \dots, N \quad (4b)$$

Without loss of generality, suppose that  $\omega_1 = \omega_2 = \dots = \omega_r = \omega_0$  is a repeated frequency with its multiplicity equal to  $r$ . In order to obtain the governing equation corresponding to this repeated frequency in modal coordinates,  $\eta_0(t) = \{\eta_{01}(t), \eta_{02}(t), \dots, \eta_{0r}(t)\}^T$ , we can rewrite Eq. (3) in the partitioned form

$$\begin{bmatrix} \ddot{\eta}_0(t) \\ \vdots \\ \ddot{\eta}_d(t) \end{bmatrix} + \begin{bmatrix} \omega_0^2 I_r & \\ & \ddots \\ & \Omega_d^2 \end{bmatrix} \begin{bmatrix} \eta_0(t) \\ \vdots \\ \eta_d(t) \end{bmatrix} = \begin{bmatrix} \Phi_0^T \\ \vdots \\ \Phi_d^T \end{bmatrix} B u(t) \quad (5a)$$

$$y = C \begin{bmatrix} \Phi_0 & \vdots & \Phi_d \end{bmatrix} \begin{bmatrix} \eta_0(t) \\ \vdots \\ \eta_d(t) \end{bmatrix} = C \Phi_0 \eta_0(t) + C \Phi_d \eta_d(t) \quad (5b)$$

where  $\Phi_0 \equiv [\varphi_1, \varphi_2, \dots, \varphi_r]$ ,  $\Phi_d \equiv [\varphi_{r+1}, \varphi_{r+2}, \dots, \varphi_n]$ . Then the observation equation corresponding to the repeated frequency modes, denoted as  $y_0$ , can be expressed as

$$y_0 = C_0 \eta_0(t) \quad (5c)$$

and the governing equation corresponding to this repeated frequency in terms of modal coordinates  $\eta_0(t)$  can be rewritten as

$$\ddot{\eta}_0(t) + \omega_0^2 I_r \eta_0(t) = B_0 u(t) \quad (5d)$$

where  $B_0 \in R^{r \times p}$ ,  $C_0 \in R^{l \times r}$ , and  $I_r$  is the  $r \times r$  identity matrix,

$$B_0 = \Phi_0^T B \quad (5e)$$

$$C_0 = C \Phi_0 \quad (5f)$$

Since the matrices  $B_0$  and  $C_0$  contain the complete information about controllability and observability for these repeated modes, respectively, we can focus on them to investigate the controllability and observability.

### Quantitative Measure for Controllability and Observability

For the repeated frequency modal system described by Eq. (5), it is controllable if and only if<sup>4-6</sup>

$$\text{rank}(B_0) = r \quad (6)$$

and it is observable if and only if<sup>4-6</sup>

$$\text{rank}(C_0) = r \quad (7)$$

Although this criterion is true, it only provides a yes-no type answer. Furthermore it does not demonstrate the composition of this eigensubspace  $\phi_0$  in terms of its controllability and observability.

First consider how to measure the controllability of Eq. (5d) and how to find a new basis vector from this eigenspace ( $\Phi_0$ ) so as to more clearly reveal the properties of controllability.

Taking the singular-value decomposition of  $B_0 \in R^{r \times p}$  yields

$$B_0 = U S V^T \quad (8a)$$

where  $U \in R^{r \times r}$ ,  $V \in R^{p \times p}$ ,  $U^T U = I_r$ ,  $V^T V = I_p$ ,

$$S = \begin{bmatrix} \Sigma & 0 \\ 0 & 0 \end{bmatrix}_{r \times p} \quad (8b)$$

and  $\Sigma = \text{diag}[\sigma_1, \sigma_2, \dots, \sigma_m]$ . Here the nonzero positive numbers  $\sigma_i$  are in descending order,  $\sigma_1 \geq \sigma_2 \geq \dots \geq \sigma_m > 0$ .

Premultiplying both sides of Eq. (8a) by  $U^T$  and recalling that  $B_0 = \Phi_0^T B$  yield

$$\bar{\Phi}_0^T B = S V^T \quad (9)$$

where

$$\bar{\Phi}_0 = \Phi_0 U \quad (10)$$

As can be seen from Eq. (10),  $\bar{\Phi}_0$  is also the modal matrix corresponding to this repeated eigenvalue  $\omega_0$ , which satisfies the orthogonality condition with respect to the mass matrix  $M$ ,

$$\bar{\Phi}_0^T M \bar{\Phi}_0 = I_r \quad (11)$$

To illustrate the information given by  $\bar{\Phi}_0$  and  $\sigma_i$  ( $i = 1, 2, \dots, r$ ) about the controllability of these repeated modes, let us introduce a new group of repeated frequency modal coordinates  $\xi = \{\xi_1, \xi_2, \dots, \xi_r\}^T$  through the following coordinate transformation:

$$x(t) = \bar{\Phi}_0 \xi(t) \quad (12)$$

Incorporation of Eq. (12) into Eq. (1) gives the governing equation and the observation equation, respectively, in terms of  $\xi(t)$  as

$$\ddot{\xi}(t) + \omega_0^2 I_r \xi(t) = \bar{\Phi}_0^T B u(t) \quad (13)$$

Substituting Eq. (9) into the right side of Eq. (13) yields

$$\ddot{\xi}(t) + \omega_0^2 I_r \xi(t) = S V^T u(t) \quad (14)$$

Equation (14) may also be written in the following form assuming that  $u'(t) \equiv V^T u(t)$ :

$$\ddot{\xi}(t) + \omega_0^2 I_r \xi(t) = S u'(t), \quad u'(t) \equiv V^T u(t) \quad (15)$$

Because as  $V_{p \times p}^T V_{p \times p} = I_p$ ,  $u(t)$  and  $u'(t)$  can be considered to be of equivalence in terms of energy required.

As can be seen from Eq. (15), the qualitative and quantitative characteristics of each repeated frequency modal coordinate  $\xi_i$  ( $i = 1, 2, \dots, r$ ) can be shown clearly:

1) The necessary and sufficient condition of the controllability of all the repeated-frequency modal coordinates  $\xi_i$  ( $i = 1, 2, \dots, r$ ) is  $\text{rank}(S) = r$  or  $p \geq r$  and  $m = r$ .

2) When  $0 < m < r$ , only a part of the repeated frequency mode coordinates is controllable, i.e.,  $\xi_i$  ( $i = 1, 2, \dots, m$ ) are controllable, leaving the rest,  $\xi_i$  ( $m + 1 \leq i \leq r$ ), uncontrollable.

3) Since  $u'(t)$  is equivalent to  $u(t)$  in terms of energy required, the controllability of  $\xi_i$  can be measured using  $\sigma_i$ . The greater  $\sigma_i$  is, the less energy is required to produce the same control effect on  $\xi_i$ . If  $\sigma_i$  is small, it will cost much more energy even to produce only a little effect on  $\xi_i$ .

The controllability is shown in a clear manner using the modal matrix  $\xi$ . We shall refer to the modal matrix  $\bar{\Phi}_0 \equiv [\bar{\varphi}_1, \bar{\varphi}_2, \dots, \bar{\varphi}_r]$  as the controllable principal modal matrix (C-PMC),  $\xi_i$  as the  $i$ th controllable principal modal coordinate (C-PMC), and the associated modal vector  $\bar{\varphi}_i$  as the  $i$ th controllable principal modal vector (C-PMV).

On the basis of duality we can find another group of repeated modal coordinates  $\rho = \{\rho_1, \rho_2, \dots, \rho_r\}^T$  under which the observable properties of Eq. (5c) possess the same clear version as well.

Taking the singular-value decomposition of  $C_0$  yields

$$C_0 = U_0 S_0 V_0^T \quad (16)$$

where  $U_0 \in R^{l \times l}$ ,  $V_0 \in R^{r \times r}$ ,  $U_0^T U_0 = I_l$ ,  $V_0^T V_0 = I_r$ ,

$$S_0 = \begin{bmatrix} \Sigma & 0 \\ 0 & 0 \end{bmatrix}$$

and  $\Sigma_0 = \text{diag}(\sigma_{01}, \sigma_{02}, \dots, \sigma_{0k})$ ,  $\sigma_{01} \geq \sigma_{02} \geq \dots \geq \sigma_{0k} > 0$ . Taking coordinate transformation of Eq. (1) into coordinate  $\rho(t)$  through

$$x(t) = \Psi_0 \rho(t) \quad (17)$$

where

$$\Psi_0 \equiv \Phi_0 V_0 \quad (18)$$

we can obtain

$$y_0 = C \Psi_0 \rho(t) \quad (19)$$

As can be seen from Eq. (18),  $\Psi_0$  is also the modal matrix associated with the repeated frequency  $\omega_0$  and satisfies  $\Psi_0^T M \Psi_0 = I_r$ . Therefore  $\rho(t)$  is also the modal coordinate corresponding to  $\omega_0$ .

Recalling that  $C_0 = C \Phi_0$ , Eq. (19) can be rewritten as

$$y_0 = C_0 V_0 \rho(t) \quad (20)$$

Substituting Eq. (16) into Eq. (20) finally yields

$$y_0 = U_0 S_0 \rho(t) \quad (21)$$

Define a quantitative measure for the amplitude of output  $y_0$  as

$$J_0 \equiv y_0^T y_0 \quad (22)$$

Substituting Eq. (21) into Eq. (22) yields

$$J_0 = \rho(t)^T S_0^T S_0 \rho(t) = \sum_{j=1}^k \sigma_{0j}^2 \rho_j^2(t) \quad (23)$$

As can be seen in Eq. (23), the qualitative and quantitative characteristics of each repeated frequency mode coordinate  $\rho_i(t)$  ( $i = 1, 2, \dots, r$ ) can be shown clearly:

1) The necessary and sufficient condition for the observability of all the repeated frequency mode coordinates  $\rho_i(t)$  ( $i = 1, 2, \dots, r$ ) is that  $\text{rank}(S) = r$  or  $l \geq r$  and  $k = r$ .

2) When  $0 < k < r$ , only the coordinates  $\rho_i(t)$  ( $i = 1, 2, \dots, k$ ) are observable, leaving the other  $\rho_i(t)$  ( $k+1 \leq i \leq r$ ) unobservable.

3) The observability of  $\rho_i(t)$  ( $i = 1, 2, \dots, k$ ) can be measured using  $\sigma_{0i}$ . The greater  $\sigma_{0i}$  is, the more  $\rho_i(t)$  weighs in  $J_0$ . If  $\sigma_{0i}$  is small,  $\rho_i(t)$  will not dominate in  $J_0$  even if the magnitude of  $\rho_i(t)$  itself is large.

Due to the simple and clear version of the observability property under the modal coordinates  $\rho(t)$ , we call the modal matrix  $\Psi_0$  ( $\Psi_0 \equiv \Phi_0 V_0 = [\psi_1, \psi_2, \dots, \psi_r]$ ) the observable principal modal matrix (O-PMM),  $\rho_i$  the  $i$ th observable principal modal coordinate (O-PMC), and the corresponding modal vector  $\psi_i$  the  $i$ th observable principal modal vector (O-PMV).

As can be seen from the above process, these two kinds of principal modes, C-PMV and O-PMV, would coincide when  $B = C^T$ .

### Numerical Example

Consider the plane truss shown in Fig. 1. Its first six natural frequencies (4.6042 rad/s) are repeated with its multiplicity equal to 6. For this example two different placements of force actuators are listed in Table 1, designated as cases 1 and 2, respectively. As can be seen from Table 1, eight actuators are used for the two cases, but the placements are different. The results of these two placements are included in Table 2.

Table 1 Placement of actuators

Case	Number of actuators	Positions at which actuators act	
		In direction X	In direction Y
1	8	At nodes 2, 4, 8, 12	At nodes 4, 8, 12, 14
2	8	At nodes 2, 4, 12, 14	At nodes 2, 4, 12, 14

Table 2 Values of controllability measures for repeated modes

Case	Dim <sup>a</sup>	$\sigma_1$	$\sigma_2$	$\sigma_3$	$\sigma_4$	$\sigma_5$	$\sigma_6$
1	6	0.12909	0.12909	0.12909	0.12909	0.091287	0.091287
2	4	0.12909	0.12909	0.12909	0.12909	0	0

<sup>a</sup>Dimension of subspace that can be controlled.

It can be seen from Table 2 that these six modes are all controllable for case 1 with the measures of controllability equal to 0.129099 and 0.091287. This implies that these six modes can all be controlled in case 1.

However, for case 2 only a subspace from these six modes is controllable, with its complementary subspace uncontrollable, since there are two zero singular values,  $\sigma_5 = \sigma_6 = 0$ . The first C-PMV of this controllable subspace is shown in Fig. 1. The C-PMV of the uncontrollable fifth mode is shown in Fig. 2. Any mode from the subspace consisting of the two C-PMVs associated with  $\sigma_5$  and  $\sigma_6$  cannot be controlled. Therefore in case 2 the controllable modes must belong to the subspace consisting of the four controllable modes, and all the uncontrollable modes must be from the subspace consisting of the two uncontrollable modes.

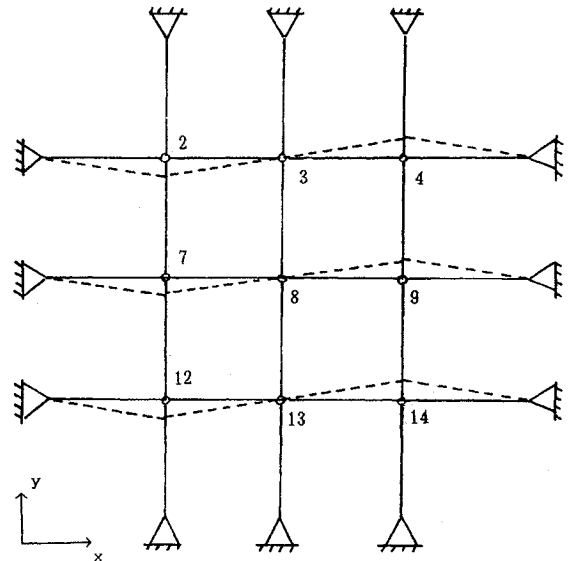


Fig. 1 First C-PMV for case 2,  $\sigma = 0.12909$ .

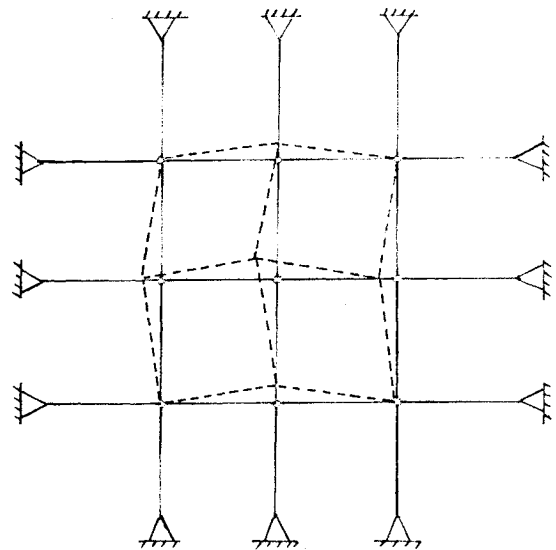


Fig. 2 Fifth C-PMV for case 2,  $\sigma = 0.00000$ .

## Concluding Remarks

The vibration control of large flexible space structures with repeated or closely spaced frequencies is a challenging problem. Most of the previous investigations have focused on the qualitative analysis. Although some criteria for model reduction, such as frequency criterion and controllability and observability criteria, have been considered in the past, they cannot deal with vibration modes with repeated frequency. The contribution of the present paper is the use of the singular-value decomposition of the input matrix  $B_0$  in defining controllability. This approach is also used to define the observability on the basis of duality. Using this method, the concepts of controllable principal modes and observable principal modes are introduced. These concepts describe the structures of controllability and observability for the subspace of the repeated-frequency modes in a more clear fashion. They are of practical importance for model reduction, sensor/actuator placement, and placement of exciters/sensors for modal parameter identification.

## Acknowledgment

This study was supported by the National Natural Science Foundation of China.

## References

- <sup>1</sup>Hamdan, A. M. A., and Nayfeh, A. H., "Measures of Modal Controllability and Observability for First- and Second-Order Linear Systems," *Journal of Guidance, Control, and Dynamics*, Vol. 12, No. 3, 1989, pp. 421–428.
- <sup>2</sup>Porter, B., and Crossley, R., *Modal Control Theory and Applications*, Taylor & Francis, 1972.
- <sup>3</sup>Laub, A. J., and Arnold, W. F., "Controllability and Observability Criteria for Multivariable Linear Second-Order Models," *IEEE Transactions on Control*, Vol. AC-29(2), 1984, pp. 163–165.
- <sup>4</sup>Hughes, P. C., and Skelton, R. E., "Controllability and Observability of Linear Matrix Second-Order Systems," *ASME Journal of Applied Mechanics*, Vol. 47, 1980, pp. 415–420.
- <sup>5</sup>Gregory, C. Z., Jr., "Reduction of Large Flexible Spacecraft Models Using Internal Balancing Theory," *Journal of Guidance Control and Dynamics*, Vol. 7, No. 6, 1984, pp. 725–732.
- <sup>6</sup>Williams, T., "Closed-Form Grammians and Model Reduction for Flexible Space Structures," *IEEE Transactions on Automatic Control*, Vol. 35, No. 3, 1990, pp. 372–382.

# Automatic Formation Flight Control

M. Pachter,\* J. J. D'Azzo,<sup>†</sup> and J. L. Dargan<sup>‡</sup>  
Air Force Institute of Technology,  
Wright-Patterson AFB, Ohio 45433

## I. Introduction

**T**HE formation flight control problem is addressed in this Note. The automatic control of a two-aircraft flight, such that the formation's initial geometry is preserved during heading change and speed change maneuvers, is considered. A typical leader/wingman "diamond" formation is considered (see Fig. 1).

From an operational point of view, and in line with the current operational practice of manually flown formation flights, it is advantageous to stipulate a leader/follower concept for automatic formation flight control. This envisages a follower, i.e., the wingman, equipped with a "formation-hold" autopilot. Thus, the wingman ( $W$ ) is controlled by the formation-hold autopilot.

Received Aug. 3, 1992; revision received March 25, 1994; accepted for publication May 23, 1994. This paper is declared a work of the U.S. government and is not subject to copyright protection in the United States.

\*Associate Professor, Department of Electrical and Computer Engineering.

<sup>†</sup>Professor and Department Head, Department of Electrical and Computer Engineering.

<sup>‡</sup>Captain, U.S. Air Force, Department of Electrical and Computer Engineering.

The aircraft are modeled as first-order dynamic systems. It is assumed that the position of the leader ( $L$ ) relative to  $W$  is available to  $W$ , and a  $W$  control system is developed for the automatic maintenance of the formation. The above-mentioned automatic formation flight control system (FFCS) is referred to as the formation-hold autopilot. Thus,  $W$  is able to maintain his or her position relative to  $L$  (station keeping), in the face of maneuvers by  $L$ . In addition,  $L$  can "command" a change ( $\Delta x_r$ ,  $\Delta y_r$ ) in the formation's parameters, i.e., a change in the  $L$ - $W$  lateral and longitudinal separation ( $x_r$ ,  $y_r$ ). This prompts the formation-hold autopilot to command  $W$  to execute a maneuver in order to effect the commanded change. Hence,  $L$  literally "leads," or drives, the formation.

Concerning the measurements available for feedback, it is imperative that the perturbations in  $W$ 's position in the formation,  $x$  and  $y$ , be available to the  $W$  collocated formation-hold autopilot. The additional information of heading error and speed error, viz., the availability of the measurements of leader-wingman heading and speed differentials, significantly improve the formation-hold autopilot's performance.

An early U.S. Army formation flight control system feasibility study was conducted in 1965. It concluded that a FFCS would relieve the pilot of the burdensome tasks required during formation flight and would greatly enhance formation flying performance (Ref. 1, p. 148). Recently, a preliminary FFCS study was performed by Rohs,<sup>2</sup> who considered diamond and trail formations of like and dissimilar aircraft. The work presented herein is based on the thesis research performed by Dargan<sup>3</sup> and Dargan et al.<sup>4</sup> In the present paper, a rotating frame of reference, affixed to  $W$  instantaneous position, is employed. The formation control problem is then modeled by a nonlinear dynamic system, which is developed in Sec. II. In Sec. III, the dynamic system is linearized about its initial steady-state condition. A decomposition principle is at work in the FFCS, which greatly facilitates the synthesis of the linear proportional-plus-integral (PI) controller. The crucial decomposition of the FFCS is performed in Sec. IV, followed by the analysis of the  $y$  and  $x$  channel control systems in Sec. V. The decomposition-based control design concept is very much in line with Porter and Bradshaw's modal (decomposition) method.<sup>5,6</sup> Finally, the linear plant model is employed to design a linear PI wing controller, which is the formation-hold autopilot. The formation-hold control concept is illustrated in Fig. 2 in Sec. V. The performance of the formation-hold autopilot is gauged by exercising the simulation with maneuvers performed by  $L$  (e.g., changes in  $L$  heading and speed). In addition, changes in the formation's parameters and formation changes can be commanded. An example of these simulation results is presented in Sec. VI. Concluding remarks are contained in Sec. VII.

## II. Formation Flight Control Modeling

### A. Main Assumptions

In the formation flight control problem analysis, it is tacitly assumed that standard autopilot loops have been closed around each aircraft in the formation. Hence, the aircraft are "flown" by controlling their respective Mach-hold and course-hold autopilots' reference signals.

### B. Aircraft Dynamics

It is thus assumed that the following two decoupled autopilots are in place: (1) heading-hold autopilot, which accepts a (small) heading change command  $\psi_c$  in the heading  $\psi$  without affecting the aircraft's airspeed, and (2) Mach-hold autopilot, which accepts a (small) speed change command  $\Delta V_c$  in speed  $V$  without affecting the aircraft's altitude. These decoupling assumptions implicitly presuppose coordinated throttle, stick, aileron, and rudder control in the first autopilot and coordinated stick and throttle control in the second autopilot. Furthermore, the heading dynamics and the attendant speed response of the autopilot controlled  $L$  and  $W$  aircraft are first order, respectively. Finally, realism-enhancing rate saturation nonlinearities are included in the above models.

The (linearized) dynamics are

$$\dot{\psi}_W = -\frac{1}{\tau_{\psi_W}} \psi_W + \frac{1}{\tau_{\psi_W}} \psi_{Wc} \quad (1)$$